Alkaline Electrolyzer and V2G System DIgSILENT Models for Demand Response Analysis in Future Distribution Networks

Iker Diaz de Cerio Mendaza, *Student-Member*, *IEEE*, Birgitte Bak-Jensen, *Senior-Member*, *IEEE*, and Zhe Chen, *Senior-Member*, *IEEE*
Department of Energy Technology, Aalborg University
Pontoppidanstræde 101, 9220, Aalborg Ø, Denmark
idm@et.aau.dk

***Abstract*— Grid instabilities originated by unsteady generation, characteristic consequence of some renewable energy resources such as wind and solar power, claims for new power balance solutions in largely penetrated systems. Denmark's solid investment in these energy sources has awaked a need of rethinking about the future control and operation of the power system. A widespread idea to face these challenges is to have a flexible demand easily adjustable to the system variations. Electro-thermal loads, electric vehicles and hydrogen generation are among the most mentioned technologies capable to respond, under certain strategies, to these variations. This paper presents two DIgSILENT PowerFactory models: an alkaline electrolyzer and a vehicle to the grid system. The models were performed using DIgSILENT Simulation Language, aiming to be used for long-term distribution systems simulations. Two voltage levels were considered: 20 kV for the electrolyzer grid connection and 0.4 kV for the plug-in electric vehicle. Simulation results illustrate the simplicity and manageability of the presented models.**

***Index Terms*—Alkaline Electrolyzer, V2G system, Demand Side Management, Smart Grids, DIgSILENT PowerFactory.**

I. Introduction

Denmark has actively supported sustainable development and renewable energy integration during the last decades. Wind power has specially suffered an extraordinary growth reaching 21.3% of the total share in 2010. In March 2012, the Danish Ministry of Climate, Energy and Building accelerated the renewable energy targets set by previous energy plans. The wind power is introduced as the primary electricity supply source in 2020, expecting to cover 50% of the national electrical consumption [1].

Considering grid instabilities and power unbalances introduced by this alternative generation the management of largely penetrated power systems becomes rather defiance. On January 2005 in the Danish offshore wind farm Horns Rev 1, a storm event resulted in zero power production from the whole park in less than five minutes. A sudden power loss of about 135 MW was originated from the shutdown of the 91 wind turbines of the wind park due to exceeding over-speed limit [2].

The strong grid interconnection with neighboring countries is a well exploited tool for regulating the actual system. This provides an extra degree of actuation to the transmission system operator (TSO) which is capable to import or export energy, depending on the instantaneous need, to keep the system frequency within the permitted limits. Despite of having plans to increase this interconnection capacity in Denmark, the future power exchange capability threatens to be drastically affected if the surrounding countries follow the same ambitious targets as Denmark. For that reason, local energy management using active control of loads is becoming a popular idea to mitigate the impact from the renewables in the power system. The Danish IDA Climate Plan defines a close interaction among the future electric, heating and transportation systems, including also the electrolysis as a possible alternative for fuel generation [3].

The following paper presents two DIgSILENT PowerFactory models: an alkaline electrolyzer (AE) and a vehicle to the grid (V2G) system. The aim is to assess their power regulation potential and their impact in future distribution systems by long-term simulations.

The literature regarding their modelling is wide; being possible to find different ways and types of models depending on the analysis required. A detailed AE model was properly introduced by Ulleberg [4], [5], dividing its structure in three main parts; I-U characteristic, thermal model and the hydrogen production. Its influence was posteriorly assessed inside a renewable energy based stand-alone power system, stating its good accuracy and suitability for this kind of system analysis. Authors in [6] used the previous work to model different electrolyzers for different hybrid system applications. Battista et al. [7] employed the von Hoerner system in order to address the power control of a wind-hydrogen system. Based also in this last one, a more simplified model was introduced by Onar et al. [8] for dynamic simulations in a wind/fuel cell/electrolyzer/ultra-capacitor system. His implementation may be restricted due to the consideration of

The authors would like to thank the Danish Council for Strategic Research for providing the financial support for the project Development of a Secure, Economic and Environmentally-friendly Modern Power Systems (DSF 09-067255).

constant temperature and operation point.

Concerning the plug-in electric vehicle (PEV) storage, lithium-ion and lithium ion polymer batteries are commonly used technologies due to their long life cycle, high power and energy density characteristics. The classification made by Chen and Rincon-Mora [9] shows that the electrical battery models are the most relevant for grid studies. Detailed lithium-ion battery models were introduced by authors in [10], [11] focusing in representing accurately their dynamic behaviour during charge and discharge periods. The representative electrical parameters were obtained via experimental tests and analytically defined as a polynomial regression. Aggregated and more simplified models were used by authors in [12], [13] instead, focusing on the load frequency response in power system analysis.

The authors intend to study the interaction of these two loads in local distribution networks. The lack of information on how to implement them in an analysis tool like DIgSILENT PowerFactory, motivate to address this issue in this manuscript.

The paper is divided in the seven sections. Section I gives a short introduction about the problem statement and the state of the art. Through section II, the AE and the V2G system models are described. In section III their implementation using DIgSILENT Simulation Language (DSL) is introduced. Section IV presents the obtained simulation results. Finally Section V and VI provide the conclusions and references.

II. Unit Modelling

A. Alkaline Electrolyzer

An AE is the combination of different electro-mechanical elements, which allows the decomposition of an electrolyte -solution of KOH in water- into hydrogen and oxygen, by passing a direct current between two electrodes.

$$H_2O(l) + Electrical\ energy \rightarrow H_2(g) + \frac{1}{2}O_2(g) \quad (1)$$

It can be considered as a mature technology in comparison with proton exchange membrane (PEM) and solid oxide electrolysis (SOE), wherefore it is commonly used in large scale hydrogen production applications. A simplified grid connection topology of a large AE in a distribution network is shown in Fig.1(a).

As an essential reference in the AE modelling, the work published by Ulleberg [5], must be stated. As he introduced three sub-parts delimited AE model structure: I-U characteristic curve for an AE cell, thermal model and hydrogen production. In Fig.1(b) is also included the compressor model.

1) I-U Characteristic Curve: The following non-linear equation, proposed by Ulleberg [5], represents the current and voltage kinetics in the electrode. This expression, including the overvoltage dependence on the temperature resulting from the chemical reactions, was obtained from empirical results.

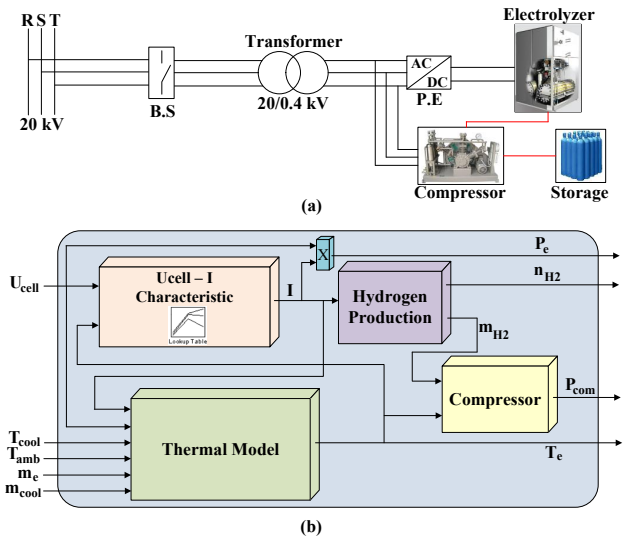

Fig. 1. Alkaline Electrolyzer: (a) Simplified grid connection lay-out and (b) Model structure.

$$U_{cell} = U_{rev} + \frac{r_1 + r_2 T_e}{A_{cell}} I + (s_1 + s_2 T_e + s_3 T_e^2) log(\frac{t_1 + t_2/T_e + t_3/T_e^2}{A_{cell}} I + 1) \quad (2)$$

$$U_e = n_c U_{cell} \quad (3)$$

where U_e is the electrolyzer voltage and n_c the number of cells, U_{cell} is the voltage of a cell and U_{rev} the reversible voltage, r_i are the parameters for ohmic resistance of electrolyte (i=1…2), s_i and t_i are parameters for overvoltage on electrodes (i=1…3), A is the cell area, T_e is the electrolyte temperature and I is the DC current drawn by the AE. The model parameters and coefficients are listed in the Table I.

For an operational pressure of 7 bars, similar as the system installed at Jülich (PHOEBUS), the curves developed from the above expression are presented in the Fig.2. Hereof a two dimensional matrix (look-up table) was created with the purpose of defining the current drawn by the AE, according to T_e and U_e applied in the stack.

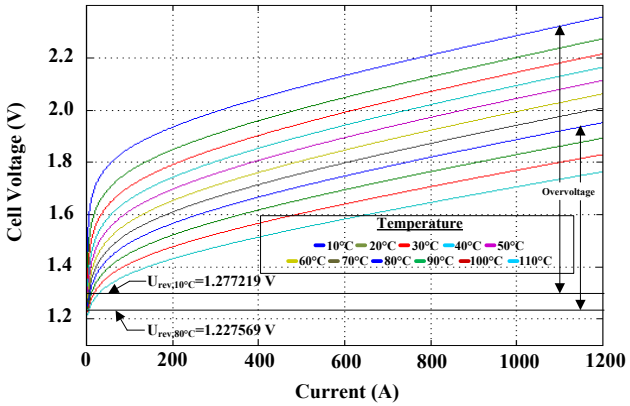

Fig. 2. I-U characteristic curve for the modelled AE cell at operating pressure of 7 bar

The thermodynamics of the electrochemical reactions is an important factor to be taken into account. The changes in enthalpy (ΔH) and entropy (ΔS) of the water splitting reaction induce changes in Gibbs energy (ΔG) and consequently in the U_{rev}. These parameters are directly affected by the working conditions of the AE (operation pressure and temperature).

$$U_{rev} = \frac{\Delta G}{zF} = \frac{\Delta H - T_e \Delta S}{zF} \tag{4}$$

where z is the number of electrons transferred per reaction (z=2) and F is the faraday constant (∼96485 C/mol). The changes in Gibbs energy was calculated as described in [14], using the thermodynamic properties of products and reactants obtained from the NIST online database. Then, for the operating pressure of 7 bars, a polynomial regression was made in order to define U_{rev_7bar} as function of T_e.

$$U_{rev\_7bar} = -2.483e^{-10}T_e^3 + 2.9004e^{-7}T_e^2 - 0.000733T_e + 1.2845 \tag{5}$$

2) Thermal Model: The temperature variation of the electrolyte, during the hydrolysis, can be represented by a thermal energy balance as the following differential equation states.

$$C_t \frac{dT_e}{dt} = Q_{gen} - Q_{cool} - Q_{loss} \tag{6}$$

where C_t is the thermal capacitance of the AE. The internal heat generation (Q_{gen}) is a consequence of the cell inefficiencies and is directly related with the power consumed by the AE (P_e) and the electrolysis efficiency (η_e). This latter one can be expressed as the quotient between the thermo-neutral voltage (U_{th}) and U_{cell}.

$$Q_{gen} = P_e(1-\eta_e) = P_e(1-\frac{U_{th}}{U_{cell}}) = n_c(U_{cell}-U_{th})I \tag{7}$$

$$U_{th} = \frac{\Delta H}{zF} \tag{8}$$

The U_{th} defines a voltage threshold for the heat release in the process. If this value is exceeded the heat released becomes higher than the required for the water decomposition increasing the accumulated heat in the stack and resulting in temperature increases. Again, a polynomial regression was made to represent U_{th} as function of T_e for an operating pressure of 7 bars.

$$U_{th\_7bar} = -3.2084e^{-10}T_e^3 + 5.4591e^{-8}T_e^2 - 0.000165T_e + 1.485 \tag{9}$$

The heat released as losses (Q_{loss}) is expressed as the difference between the T_e and the ambient temperature (T_{amb}) divided by the overall thermal resistance (R_t). Based on the parameterization of [5] and the difficulties finding real characteristic data, values of R_t and C_t were scaled up to achieve a logical thermal behaviour on this unit size.

$$Q_{loss} = \frac{1}{R_t}(T_e - T_{amb}) \tag{10}$$

The cooling is a critical issue if an accurate response and control of the AE is required. Among the different cooling methods, circulating the electrolyte through a heat exchanger is a simple and commonly used technique. The cooling demand (Q_{cool}) was calculated via the number of transfer units (ε-NTU) method, where ε is the heat exchanger effectiveness and Q_{max} the maximum theoretical cooling demand.

$$Q_{loss} = \varepsilon \cdot Q_{max} \tag{11}$$

The maximum and minimum heat capacity rates (C_{min} and C_{max}), i.e. the mass flow rate (m_e and m_{cool}) by the specific heat (c_{P_e} and $c_{P_{cool}}$), are calculated according to eq.(12) and in consequence the maximum heat (Q_{max}) with eq.(13).

$$C_{min} = \begin{cases} m_e \cdot c_{p_e} & \text{if } m_e \cdot c_{p_e} < m_{cool} \cdot c_{p_{cool}} \\ m_{cool} \cdot c_{p_{cool}} & \text{if } m_e \cdot c_{p_e} \geq m_{cool} \cdot c_{p_{cool}} \end{cases}$$

$$C_{max} = \begin{cases} m_{cool} \cdot c_{p_{cool}} & \text{if } m_e \cdot c_{p_e} < m_{cool} \cdot c_{p_{cool}} \\ m_e \cdot c_{p_e} & \text{if } m_e \cdot c_{p_e} \geq m_{cool} \cdot c_{p_{cool}} \end{cases} \tag{12}$$

$$Q_{max} = C_{min}\Delta T_{max} = C_{min}(T_e - T_{cool}) \tag{13}$$

In agreement with the methodology, ε depends on of the heat capacity ratio (C_r) and NTU coefficient, being the latter one defined as the quotient of the overall heat transfer coefficient of the heat exchanger (UA_{hx}) and C_{min}.

$$\varepsilon = \frac{1 - e^{NTU(1-C_r)}}{C_r - e^{NTU(1-C_r)}};\ NTU = \frac{UA_{hx}}{C_{min}}, C_r = \frac{C_{min}}{C_{max}} \tag{14}$$

3) Hydrogen Production: The hydrogen production rate (n_{H_2} in mol/s) is directly proportional to the current drawn by the AE stack and the number of cells connected in series.

$$n_{H_2} = \eta_F \frac{n_c I}{zF} \tag{15}$$

The faraday efficiency (η_F) represents the difference between the actual hydrogen production and the maximum theoretically talking.

$$\eta_F = a_1 \exp\left(\frac{a_2 + a_3 T_e}{I/A_{cell}} + \frac{a_4 + a_5 T_e}{(I/A_{cell})^2}\right) \tag{16}$$

4) Compressor Model: The required compression power (P_{com}) in these systems is not a power demand which can be easily dismissed, since it stands for a notable part of the total system demand. Based on the hydrogen mass flow rate (m_{H_2} in kg/s), the P_{com} was modelled assuming the compression process as polytrophic (γ=1.4) and the hydrogen as ideal gas.

$$P_{com} = m_{H_2}(W_1 + W_2) \tag{17}$$

The compression was made in two stages with an intercooling, to reduce the output temperature of the gas from the first stage to the initial temperature T_e, so the compression work in each stage was [15]:

$$W_1 = \frac{c_{p_{H_2}} T_1}{\eta_G}\left(\left(\frac{P_x}{P_1}\right)^{\gamma-1/\gamma} - 1\right)$$
$$W_2 = \frac{c_{p_{H_2}} T_1}{\eta_G}\left(\left(\frac{P_2}{P_x}\right)^{\gamma-1/\gamma} - 1\right) \tag{18}$$

where $c_{P_{H_2}}$ is the specific heat of the hydrogen and η_G is the global efficiency of the compression process. The input hydrogen pressure and temperature values (P_1, T_1) were assumed equal to AE operation conditions. The intermediate compression pressure (P_x) was calculated as the square root of P_1 and the storage pressure (P_2).

$$P_x = \sqrt{P_1 \cdot P_2} \tag{19}$$

The reactive power consumed by the induction motor driving the compressor was calculated considering a constant power factor of 0.88. Some of the stated assumptions taken in this model, especially the scaling up of C_t and R_t, could represent a limitation in some precise studies, requiring a deeper analysis on them. However, in this case the considered conditions seem to be realistic for the purposed pursued.

TABLE I
ALKALINE ELECTROLYZER MODEL

	Parameter	Quantity
General	Rated Power (kW)	355
	Operation Pressure (bar)	7
	N° of Cells	180
	Max. DC voltage (V)	342
	Min. DC voltage (V)	257.4
	Max. Opert. Temp. (°C)	80
Cell I-U Curve	$r_1(\Omega/m2)$	$7.331e^{-5}$
	$r_2(\Omega/m^2)$	$-1.107e^{-7}$
	$s_1(V)$	$1.586e^{-1}$
	$s_2(V/°C)$	$1.378e^{-3}$
	$s_3(V/°C^2)$	$-1.606e^{-5}$
	$t_1(m^2/A)$	$1.599e^{-2}$
	$t_2(m^2/A°C)$	-1.302
	$t_3(m^2/A°C^2)$	$4.213e^2$
	A (m^2)	0.25
Faraday Efficiency	$a_1(\%)$	99.5
	$a_2(m^2/A)$	-9.5788
	$a_3(m^2/A°C)$	-0.0555
	$a_4(m^4/A)$	1502.7083
	$a_5(m^4/A°C)$	-70.8005
Thermal Model	R_t(°C/W)	0.334
	$C_t(J/°C)$	5.38e6
	$UA_{hx}(W/°C)$	2100
	$m_{cool}(kg/s)$	1.2
Compressor	Rated Power (kW)	70
	N° of Stages	2
	η_G (-)	0.486
	P_2 (bar)	150

B. V2G System

The V2G concept is defined as the ability from widespread controlled PEV-s to exchange electricity with the power grid in a bidirectional way, supplying or drawing, in order to meet occasional need for stabilization. The modeled system focuses on representing the steady state behavior of a PEV connected at household level. The battery is capable to respond, under certain state of charge (SOC) limits, to a demand response control (DRC) signal sent from the local control center. Moreover the energy exchange during the hours that the vehicle is not connected at home was also taken in to account. Fig.4 shows the model structure with three parts easily differentiable.

1) Battery Model: The characteristics of the li-ion cell provided by [16] served as a reference for the following model, using the extended Thevenin battery approach to analyse its steady state behaviour within the low voltage grid. For that reason the transient dynamics were neglected, i.e the charge and discharge effects were represented only as a two different internal resistors ($R_{int,cha}$, $R_{int,dis}$). In that case the power (P_{batt}) and voltage (V_{batt}) of the battery were determined as the following equations state:

$$P_{batt} = (V_{batt} \cdot I_{batt})_{DC} \tag{20}$$

$$V_{batt} = \begin{cases} n_{cells}(V_{oc} + R_{int,cha} I_{batt}) & \text{if } I_{batt} > 0 \\ n_{cells}(V_{oc} + R_{int,dis} I_{batt}) & \text{if } I_{batt} < 0 \end{cases} \tag{21}$$

where n_{cells} is the number of cells connected in series, V_{oc} is the open circuit voltage of the cell (Fig.3(a)) and I_{batt} is the current running through the battery. The sources for this current are two, from a charging point at home (I_{HCP}) and from the energy exchanged in out-home hours (I_{OHEE}).

$$I_{batt} = I_{HCP} + I_{OHEE} \tag{22}$$

The α coefficient (Fig.3(b)) represents the charge/discharge (C/D) rate dependence on the battery cell capacity (C_{bc}) and V_{oc}, assuming negligible the temperature effect. Therefore, the SOC and the depth of discharge (DOD) were calculated as:

$$SOC = \frac{1}{C_{bc} \cdot 3600} \begin{cases} \int I_{batt} \alpha \cdot dx & \text{if } I_{batt} < 0 \\ \int \frac{I_{batt}}{\alpha} \cdot dx & \text{if } I_{batt} > 0 \end{cases} \tag{23}$$

$$DOD = DOD_{MAX} - SOC \tag{24}$$

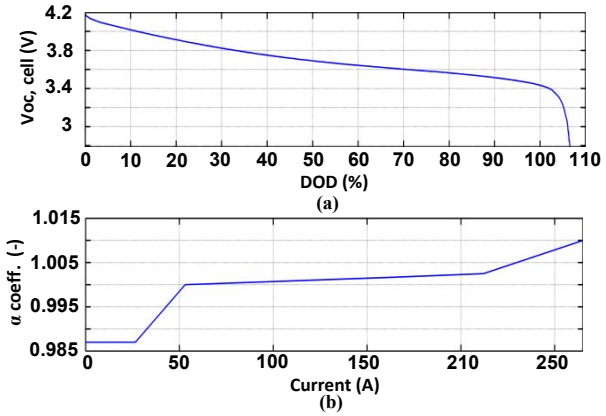

Fig. 3. Kokam SLPB 120216216 53Ah cell: (a) V_{oc} vs DOD curve (b) α coeff. vs I_{batt}.

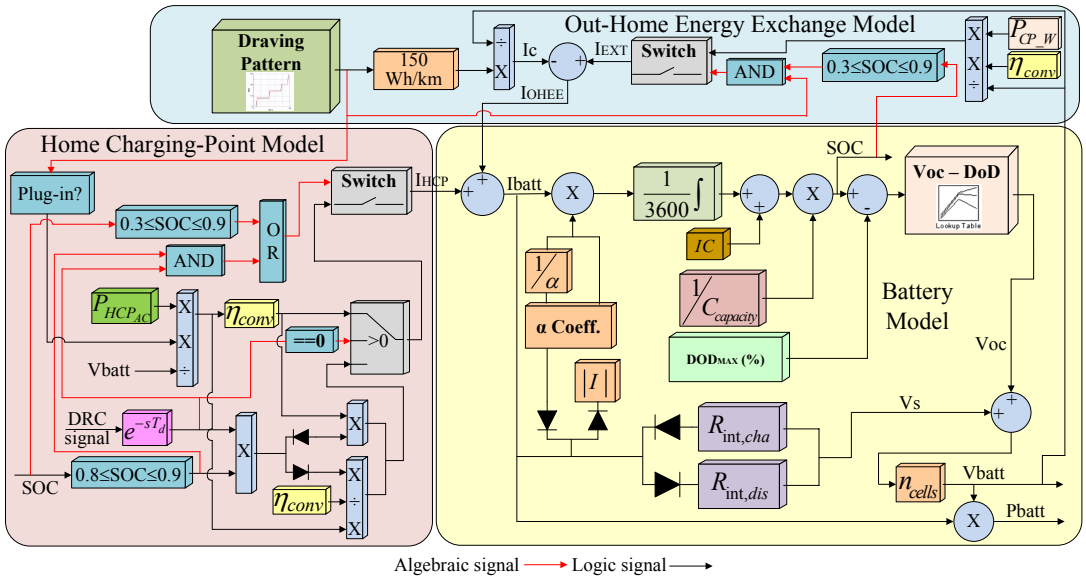

Fig. 4. V2G sytem model structure.

2) Home Charging Point Model: In local distribution networks the battery-grid-battery power exchange is highly limited by the domestic infrastructure. The V2G system capability is constrained even if the battery design allows higher power rate management. Among the different options proposed in the literature, authors found suitable the three phase connection for the Danish case and interesting for this scope.

The control of the switch, which connects and disconnects the load, is based on SOC conditions and the demand response requirements stated below. In order to avoid inconveniences for the user, the V2G system is only allowed to respond within the 80 to 90% range of the SOC. η_{conv} represents the efficiency of the AC/DC conversion and vice versa.

$$\begin{cases} C : P_{HCP} \cdot \eta_{conv} & \text{if } 0.3 > SOC > 0.9 \\ C : P_{HCP} \cdot \eta_{conv} \cdot DRC & \text{if } 0.8 > SOC > 0.9 \\ D : \dfrac{P_{HCP}}{\eta_{conv}} \cdot DRC & \text{if } 0.8 > SOC > 0.9 \end{cases} \quad (25)$$

3) Out-Home Energy Exchange Model: The SOC variations created during the periods in which the vehicle is not plugged at home were represented by the charge/discharge current I_{OHEE}. This may have different sources as well; i.e the driving energy consumption (I_c) or the plugging in external points like work place, supermarket (I_{EXT}). The current drawn from the battery during a daily trip was deducted from the vehicle driving profile -in terms of speed v (km/h)- and the V_{batt}, taking in to account an average energy consumption of 150 Wh/Km.

$$I \simeq \frac{v \cdot 150}{V_{batt}} \quad (26)$$

On the other hand, the charging mode was only taken into account for plugs in external points.

TABLE II
V2G SYSTEM MODEL

	Parameter	Quantity
Battery System	Capacity (kWh)	25
	P_{max} allowed (kW)	28.27
	N° of Cells(-)	127
	SOC Limits (-)	0.3<SOC<0.9
Cell Characteristics	Manufacturer	Kokam
	Model	SLPB 120216216
	Technology	Li-Ion
	Capacity (Ah)	53
	Voltage Range (V)	4.197-2.717
	Nom. Current (A)	53 (1C)
	$R_{int,cha}$ (mΩ)	1.3
	$Rint,dis$ (mΩ)	3.69
Charging Station	Rated Power (kW)	11
	Grid Connection	3-phase
	AC voltage (V)	400
	AC current (A)	16
	η_{conv} (-)	0.99

III. IMPLEMENTATION

DIgSILENT PowerFactory is known as a highly sophisticated power system analysis software that allows a wide range of modelling, analysis and simulation options. The implementation work was carried out using the DSL graphical interface considering the load behaviour respect to the grid as a PQ approach. In this context the technical documentation "General Load Model", available in the software help menu, turned to be a reliable source of information.

In both models, the block definition (*.BlkDef) is the start-up point for this commitment. The algebraic and differential

equations introduced in the previous section, are assigned to each block with the purpose of representing the physical behaviour of the load. As different blocks interact within each other a "Block Diagram" element is created to set and organize these relationships. The next step is creating the common models (*.ElmDsl) out of the block diagrams and other required blocks. These are recommended to be placed inside the project grid folder, accessible from the data manager window. Another important task in this phase is the parameterization and the value assignation of the data matrix-s. Finally, with the composite model (*.ElmComp) the different DSL model sub-parts are concatenated together, closing this process down.

A. Alkaline Electrolyzer

Fig.5 intends to give an overview of what has been described before referenced to the AE case. In that graphical representation it is possible to distinguish some of the procedure phases, i.e. the I-U characteristic block definition, highlighted in orange colour. The AE Plant and Load Control are represented by block diagrams in blue and green colours respectively. On the one hand, the AE Plant comprises the I-U Characteristic, Thermal Model, H2 Production and H2 Compressor single blocks which are linked by commonly shared variables. On the other hand, the Load Control block diagram content the power and refrigeration controls. The response and performance expected from AE is dependent on its operation conditions. The operation temperature and the power consumption are essential variables that need to be precisely controlled in order to have a complete regulation capacity of the unit.

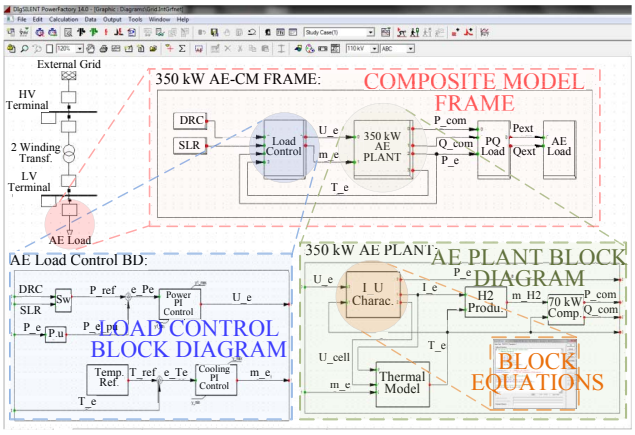

Fig. 5. AE DIgSILENT model representation.

Mechanical, power density and voltage limitation aspects induced the fact of setting the operation temperature at 80°C. The AE operation is controlled acting over two features, the power drawn from the grid and the amount of cooling provided to the unit.

Therefore, a PI determines the electrolyte recirculation mass flow rate (m_e) needed to fulfil the refrigeration requirements and achieving the temperature conditions set by the reference. An additional PI is implemented in parallel acting over the DC voltage applied in the unit terminals with the purpose of having direct control over the power consumption. The large time constant, a natural characteristic of a control variable like the temperature, results in a very slow response compared with that of the power. Thus, even existing a strong dependency between the power consumption and the operation temperature, the temperature variations are so slow that the power control dynamics are barely affected.

Finally in red colour, the composite model frame concatenates the "Load Control" and "AE Plant" block diagrams, the linking block between the DSL model and the physical load connected to the grid and both power reference input blocks. In this study, as the monitoring and control of the grid was not taken into account, the power reference signals were simply modelled as an input array using the measurement file (*.ElmFile) function of DIgSILENT PowerFactory. Again they are recommended to be placed inside the project grid folder, accessible from the data manager window.

B. V2G System

In Fig.6 the main components of the V2G system model are graphically represented. The composite model holds the common models created out of "HC Load Control", "Out-Home Energy Exchange (OEHH)" block diagrams and the "li-ion battery" single block. It also includes the block linking the DSL model and the physical load connected to the grid, the two input signal blocks and the block connecting the switching action with the physical switch in the grid. One of the two input signals provides a daily suburban driving pattern created out of the half-trips considered in [17]. The other one reproduces the DRC signal received by the unit. Both signals were also modelled as an input array. As the green colour highlights, during the "li-ion battery" common model formation the open circuit voltage and the alpha coefficient are introduced as one dimensional matrix-s. The access is through the arrow of the common model window as the picture shows. Inside, depending on the type of functions used for defining the block behaviour, the capability of writing the data will be activated or not.

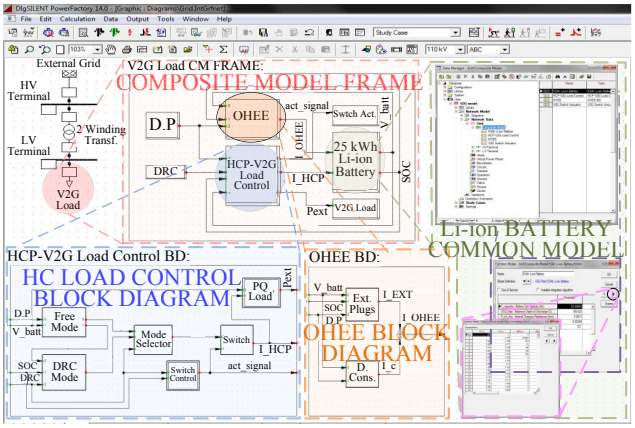

Fig. 6. V2G system DIgSILENT representation.

Concerning the control of the V2G system, already introduced in the Home Charging Point Model section, the vehicle is assumed free to be plugged whenever the user requires, acting as a normal passive load. However, as soon as it receives a DRC signal, the unit should start acting as an active and controllable load. So as to avoid dissatisfaction and unpleasant fillings from controlled users, the response capacity is constrained to an actuation range of 10%, from 80 to 90 % of the SOC. Within this range, being the vehicle plugged in the home station; the local system control centre should be capable to charge or discharge its battery in a power spectrum limited by the domestic infrastructure capacity.

IV. Results

The performance and response capability of the modelled units were investigated under several operation conditions, within a time range of a day. The point of connection (POC) of each load acquired a special interest in the performed RMS simulations for power flow, because it represents the physical union between the load and the grid.

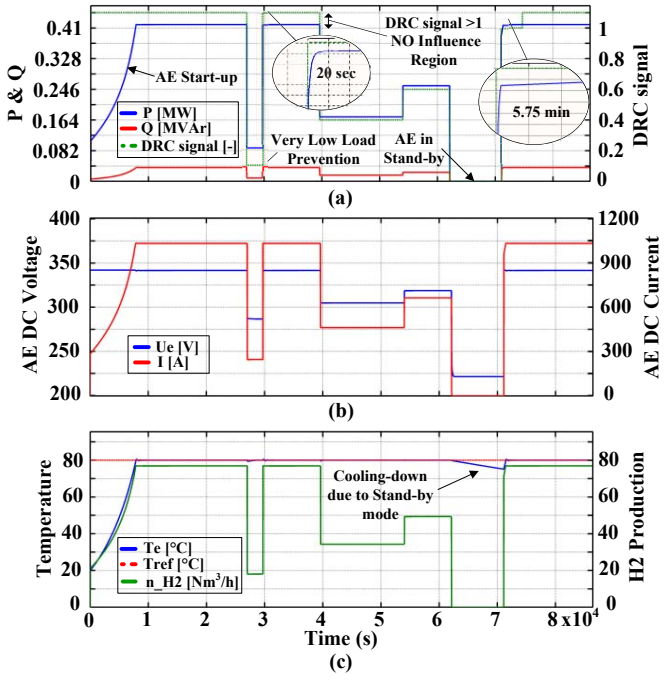

Fig. 7. AE electrolyzer simulation results: (a) P and Q consumptions messured in the POC. (b) AE voltage and current DC values. (c) AE operation temperature and H_2 production.

The AE is characterized for having long start-up times (from 0 to 100%), relatively fast downward power change dynamics and relatively slow upward power change dynamics. This is very much depending on the unit size and the accuracy, amount and availability of the cooling [18]. This may affect directly to the type of regulation that this technology can provide. Fig.7(a) shows the AE system measured active (P) and reactive power (Q) consumption at the POC. The first thing that can be noticed is the long start up time, mainly caused by the need of increasing the operation temperature. The heat generated during the electrolysis process allowed the AE slowly increasing its temperature in order to establish its rated power operation conditions. Later, a DRC signal was received forcing the AE to operate at 10% of its rated power. The down-regulation was performed very fast, in terms of seconds, but as it can be noticed the requested operation point was not possible to be achieved due to the existing limitation at low operating loads. Operating points below the 15-20% of the rated power should be avoided due to the degradation of the hydrogen purity. In this case either the AE continues operating at the stated limit or it switches into standby mode. This mode can also be forced by the DRC signal as shown later on.

In the same illustration two upward power changes are represented, one produced by the returning to the free operation mode (DRC signal>1) and the second forced by the DRC signal itself. The points from where the AE responds to the change in the operation conditions were different in each case, and so the time required for reaching the steady state condition. The reason, as Fig.7(b) shows, is the saturation of the applied DC voltage in the AE terminals, at 342V. Working within a reasonable range of cell voltages, reduces the electrical power and operation costs [4]. Therefore, after the stand-by mode period some extra time was required in order to reach the operating temperature again (Fig.7(c)).

The Li-ion battery response from the V2G model could be almost considered as instantaneous. Fig.8(a) shows the V2G system measured active power (P) consumption at the POC. For figuring out about the charging time required employing the defined connection and power level, an initial full battery charging action was simulated. A possible behaviour of the

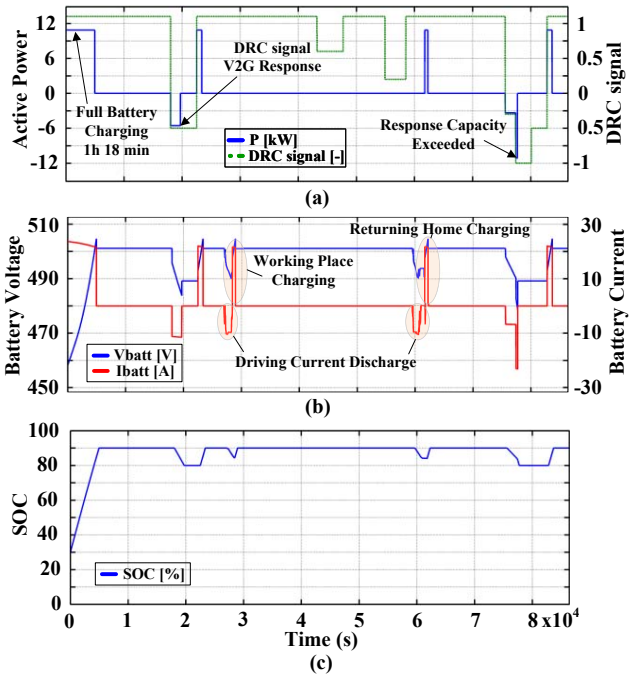

Fig. 8. V2G simulation results: (a) Active power messured in the PCC. (b) Battery voltage and current DC values. (c) State of Charge of the battery.

system was also assessed by the sending of several DRC signals to the home station along the day. In two of them (early morning and late night) the vehicle was parked and plugged at home ready to respond when the signal to discharge was received. Then, the battery started to discharge the power requested by the signal, up until the permitted SOC limit (80%). As soon as it was reached its active participation was cancelled. Time after, when the load returns to the free operation mode, it tries to recover the energy supplied previously. This effect, repeated by bunches of active loads, may lead to a serious congestion problem in certain specific grids. Another two actuation requests were also received during the analysed working day, but as the vehicle was not available at home, no respond was obtained.

Fig.8(b) gives a clear view of the battery status, in terms of voltage and currents, along the day. It is possible to recognize the current drawn during the driving periods (low, due to the vehicle speed assumed), the amount current drawn by the battery when the vehicle is plugged (at working place or at home) after a trip and the battery voltage fluctuations. Fig.8(c) shows the SOC variation for the analysed case.

V. Conclusion

This paper presents two models, an alkaline electrolyzer and a V2G system, using the dynamic simulation language DSL of DIgSILENT PowerFactory. Both are expected to be useful on impact and demand response analysis of future distribution networks. In a first place, the algebraic and differential equations describing the physical behaviour of each load were introduced. In a second stage, a detailed description of their implementation on DIgSILENT PowerFactory was given. Finally long-term power flow simulations (RMS) were carried out in order to verify their simplicity and manageability.

The obtained results show that under certain control and coordination these two flexible loads have a big potential for future power regulation activities. They are able to accommodate their operation conditions to satisfy certain requirements from the operation and control of the power system. On the other hand, certain limitations on the response speed (large AE systems) and capacity (domestic V2G system case), which may affect the future demand response strategies, have also been stated.

References

[1] Accelerating Green Energy Towards 2020. The Danish Energy Agreement of March 2012. Danish Ministery of Climate, Energy and Building, Mar. 2012.

[2] J.R. Kristoffersen, “The Horns Rev Wind Farm and the Operational Experience with the Wind Farm Main Controller”, Copenhagen Offshore Wind, 26-28 Oct. 2005.

[3] B. V. Mathiesen,“100% Renewable Energy Systems in Project Future Climate: the case of Denmark”, *in Proc. 2009 5th Dubrovnik Conference on Sustainable Development of Energy Water and Environment Systems*. Guzovic, zvonimir Duic, Neven Ban, Marko (ed.) University of Zagreb.

[4] Ø. Ulleberg, “Modeling of advanced alkaline electrolyzers: a system simulation approach”, International Journal of Hydrogen Energy. vol. 28, Issue 1, pp 21-33, 2003.

[5] Ø. Ulleberg, “Modeling Stand-Alone Power Systems for the Future: Optimal Design, Operation and Control of Solar-Hydrogen Energy Systems”, PhD Thesis, Norwegian University of Science and Technology, 1998.

[6] N. Gyawali and Y. Ohsawa, “Integrating Fuel Cell/ Electrolyzer/ Ultracapacitor System Into a Stand-Alone Microhydro Plant”, IEEE Transactions on Energy Conversion. vol.25, no.4, pp 1092-1101, 2010.

[7] H. De Battista, R.J. Mantz and F. Garelli, “Power conditioning for a windhydrogen energy system”, Journal of Power Sources 155 (2) pp 478-486, 2006.

[8] O.C. Onar, M. Uzunoglu and M.S. Alam, “Dynamic modeling, design and simulation of a wind/fuel cell/ultracapacitor based hybrid power generation system”, Journal of Power Sources, vol.161, pp 707-722, May 2006.

[9] M. Chen and G.A Rincon-Mora, “Accurate electrical battery model capable of predicting runtime and I-V performance”, IEEE Transactions on Energy Conversion, vol.21, no.2, pp. 504-511, June 2006.

[10] R.C. Kroeze and P.T. Krein, “Electrical battery model for use in dynamic electric vehicle simulations”, IEEE Power Electronics Specialists Conference (PESC), 2008 , vol., no., 15-19, pp.1336-1342, June 2008.

[11] M. Zheng; B. Qi and X. Du, “Dynamic model for characteristics of Li-ion battery on electric vehicle”, 4th IEEE Conference on Industrial Electronics and Applications (ICIEA), 2009, vol., no., 25-27, pp.2867-2871, May 2009.

[12] K. Shimizu, T. Masuta, Y. Ota and A. Yokoyama, “Load Frequency Control in power system using Vehicle-to-Grid system considering the customer convenience of Electric Vehicles”, International Conference on Power System Technology (POWERCON), 2010, vol., no., 24-28, pp.1-8, Oct. 2010.

[13] J.R. Pillai and B. Bak-Jensen, “Vehicle-to-Grid for islanded power system operation in Bornholm”, IEEE Power and Energy Society General Meeting, 2010 , vol., no., 25-29 , pp.1-8, July 2010.

[14] J.B. Jones and R.E Dugan, “*Enginnering Thermodynamics*” Prentice Hall, 1995, ISBN-10: 0023613327.

[15] J. Larminie and A. Dicks, “*Fuel Cell Systems Explained*”, 2nd Edition, John Wiley Sons, 2003, ISBN-10: 047084857X.

[16] J.V. Barreras, E. Schaltz, S.J. Andreasen and T. Minko, “Datasheet Modeling of Li-Ion Batteries”*in Proc. 2012 IEEE Vehicle Power and Propulsion Conf.* pp.830-835.

[17] S. Bashash, S. J. Moura, J. C. Forman, and H. K. Fathy, “Plug-in hybrid electric vehicle charge pattern optimization for energy cost and battery longevity”, Journal of Power Sources, vol. 196, no. 1, pp. 541-549, Jan 2011.

[18] J.O. Jensen, V. Bandur, N.J. Bjerrum, S.H. Jensen, S. Ebbesen, M. Mogensen, N. Tophj and L.Yde, ”Pre-investigation of water electrolysis, PSO-FU 2006-1-6287”, project 6287 PSO, pp. 134, 2006.